

Design and Implementation of a Millimeter Wave Active Antenna for UAV Communications

Ning Liu*, Guanfeng Cui, Guotao Shang, Ruiliang Song, and Bo Zhang

The 54th Research Institute of China Electronics Technology Group Corporation (CETC54), Beijing, China

ABSTRACT: The millimeter wave communication technology used for drones could combine the advantages of drones and millimeter waves, providing high-speed data transmission and wide area network coverage capabilities, and has broad application prospects in military and civilian communication systems. Millimeter wave active antennas have the advantages of miniaturization, high frequency band, and flexible shaping, which is of great significance for ensuring the high-speed dynamic communication ability of drone platforms. In this paper, a millimeter wave active antenna suitable for unmanned aerial vehicles (UAVs) is designed and verified, operating in 24.75–27.5 GHz and adopting Antenna in Package (AiP) design. Frequency band test and communication performance test is conducted. To open and close the RF channels, the antenna's operating frequency range can be shown in the vector network analyzer which meets the design frequency band 24.75–27.5 GHz requirements. By loading 5G millimeter wave standard signals, the antenna can achieve real-time demodulation of 100 MHz, 256QAM signals. The test shows that the system can meet the requirements of beam tracking and real-time information transmission during high-speed dynamic flight of UAVs. It has broad application prospects in UAV communication systems.

1. INTRODUCTION

The millimeter wave frequency band has shorter wavelength than traditional communication frequency bands and can support data transmission at Gbps level, meeting the development needs of high-speed and high-capacity communication systems [1]. However, the millimeter wave frequency band has higher path loss and lower scattering characteristics, resulting in higher requirements for Line of Sight (LOS) propagation conditions in millimeter wave communication systems.

Unmanned aerial vehicles (UAVs) have attracted the attention of most countries around the world due to their advantages such as low cost, simple construction, and low casualties. At present, UAVs are playing important roles in fields such as aerial photography, remote sensing and telemetry, disaster warning, and emergency communication. Due to its high flight position, UAVs often have LOS paths during communication, making them excellent platforms for millimeter wave communication. At present, the combination of millimeter wave and large-scale antenna technology to implement data communication between UAVs and ground control stations or UAVs has become a research hotspot in both academia and industry [2–5].

2. ARCHITECTURE OF THE COMMUNICATION SYSTEM

The millimeter wave system is consisted of three parts: baseband unit (BBU), active antenna unit (AAU), and user equipment (UE), as shown in Fig. 1. BBU functions as space-time scheduling, signal modulation and demodulation, channel cod-

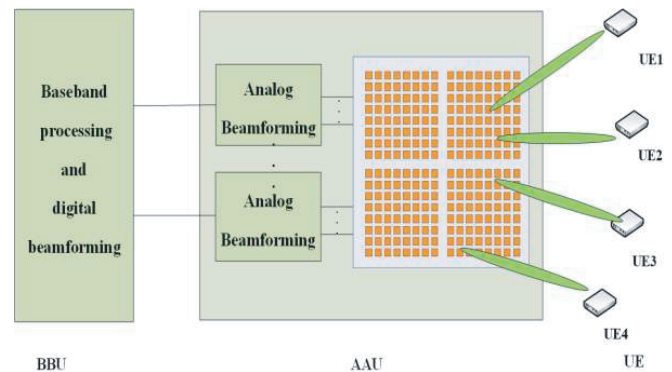


FIGURE 1. Millimeter wave system composition.

ing, signal precoding, etc. AAU functions as frequency up and down conversion, adaptive beamforming, and signal transmission and reception. UE acts the role of users. The system adopts a hybrid analog and digital beamforming architecture [6–9]. A phased array is used to replace the large number of high-speed ADC/DAC and digital processing units in the fully digital beamforming architecture. Digital precoding is carried out through a small number of digital channels to eliminate multi-user interference and achieve multi-stream transmission capability, effectively reducing the system's circuit complexity, hardware cost, power consumption, and signal processing complexity.

The number of baseband channels determines the performance of the whole millimeter-wave communication system. The more baseband channels the communication system has, the more streams simultaneously and higher peak rate it can support. On the other hand, it also affects the power consump-

* Corresponding author: Ning Liu (liuning1512@163.com).

tion and cost of the system. Taking all factors into consideration, the proposed millimeter-wave communication system adopts 4 digital channels, 256 RF channels, and 256 circularly polarized antenna elements, which are divided into 4 subarrays.

3. ACTIVE ANTENNA DESIGN

3.1. Antenna Element Design

Millimeter wave antenna elements often adopt the form of patch antennas which have small size, low profile, and are easy to implement AiP architecture design. To fully adapt to the UAV communication, circularly polarized antennas are needed [10–14]. Considering the bandwidth, polarization isolation, axial ratio, and other performance of the antenna, combined with multi-layer printed circuit board (PCB) technology, an L-shaped probe four-point feeding method is adopted in the circularly polarized antenna design [15–21]. The substrate material is TSM-DS3M, with D_k 2.94 and D_f 0.0011. The total layer of the antenna element is 12. As shown in Fig. 2, the round patch printed on the top layer is fed with an L-probe by which multiple resonance modes can be generated to extend the antenna bandwidth. The phase difference between the adjacent feeding points is 90° in the clockwise direction for the four-point feeding, which could gain good circularly-polarization performance. This antenna has excellent impedance bandwidth and circular polarization characteristics, as shown in Figs. 3 and 4. The bandwidth of voltage standing wave ratio (VSWR) and the 3 dB axial ratio exceed 20%, and the 3 dB axial ratio angle can be extended to over 160° . The maximum polarization isolation in the main radiation direction exceeds 30 dB. The overall dimension of the antenna element is $0.5\lambda \times 0.5\lambda \times 0.09\lambda$, and λ refers to the wavelength of the central frequency point, which can meet the requirements of miniaturization, low profile, and easy integration.

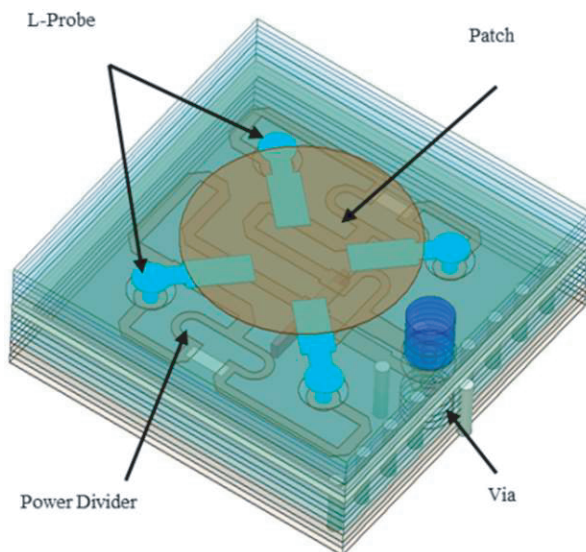


FIGURE 2. Geometry of the proposed antenna element.

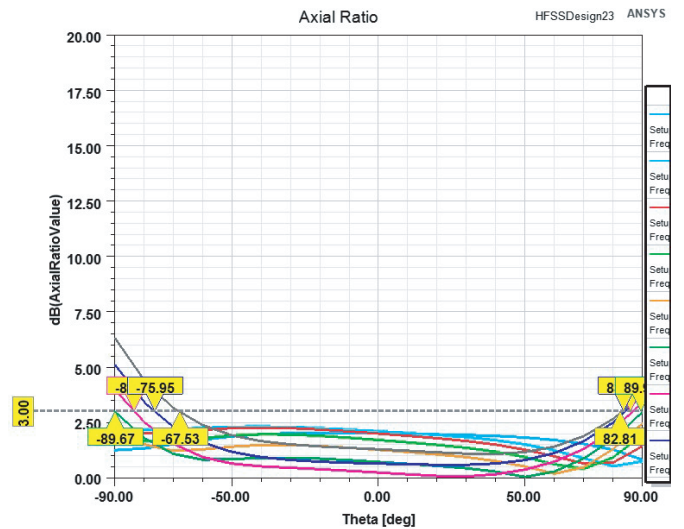


FIGURE 3. Simulation result of the radiation pattern of axial ratio.

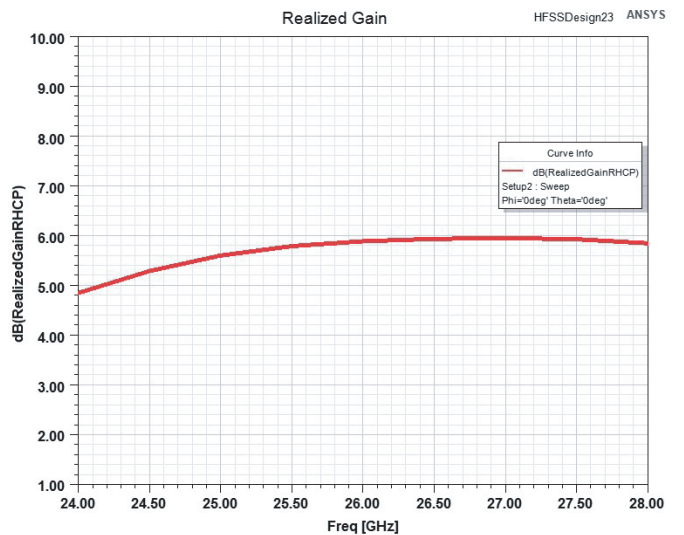


FIGURE 4. Simulation result of the realized gain against frequency of the proposed antenna element.

3.2. Antenna Array Design

To avoid the occurrence of grating lobes in phased array antennas, the spacing between the antenna elements should meet the following equation:

$$d \leq \lambda / (1 + |\sin \theta_m|) \quad (1)$$

where θ_m is the maximum scanning angle of the beam. Considering the performance requirements of the active antennas and the single channel output capability of the selected phased array TR multifunctional chip, the array layout is determined as follows:

- Arrangement: rectangular grid array.
- Channel spacing: $5.8 \text{ mm} \times 5.8 \text{ mm}$.
- Size of the antenna array: 16×16 (256 channels in total), and divided into 4 subarrays

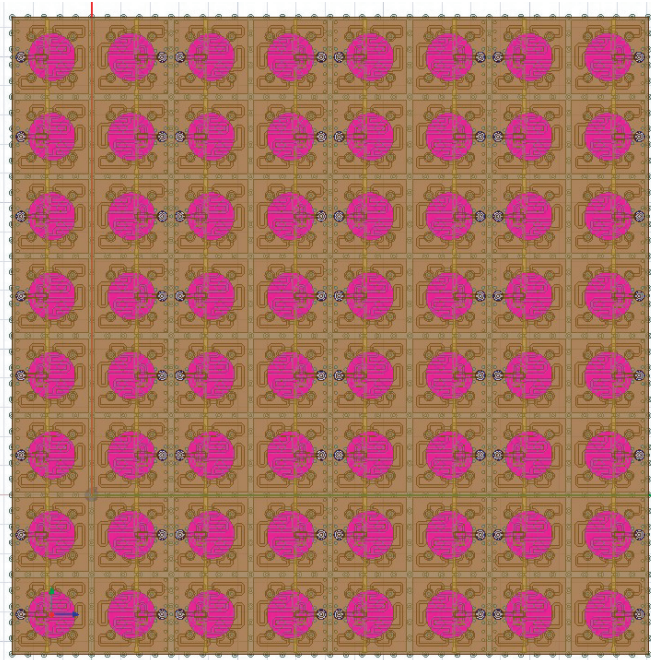


FIGURE 5. 8×8 antenna array model.

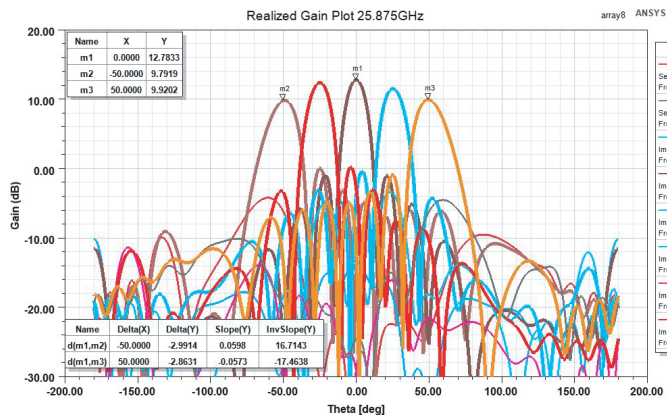


FIGURE 6. Simulation result of the scanning radiation pattern of the proposed antenna array.

The antenna array and simulation result of the scanning radiation pattern of the proposed antenna array are shown in Fig. 5 and Fig. 6.

It can be seen that the proposed 8×8 antenna array has an active VSWR of less than 1.5 and port isolation of more than 20 dB in the whole working bandwidth. When it is scanned to $\pm 50^\circ$, the gain decreases within the range of 2.8 dB. It has good impedance matching performance and beam scanning performance,.

3.3. Calibration Network Design

To satisfy the beamforming requirements, the active antennas need to have the ability of real-time calibration. The electromagnetic energy coupling method of the calibration channel is shown in Fig. 7. The radio frequency (RF) port is placed on Layer 1, and the signal is fed through coaxial to microstrip

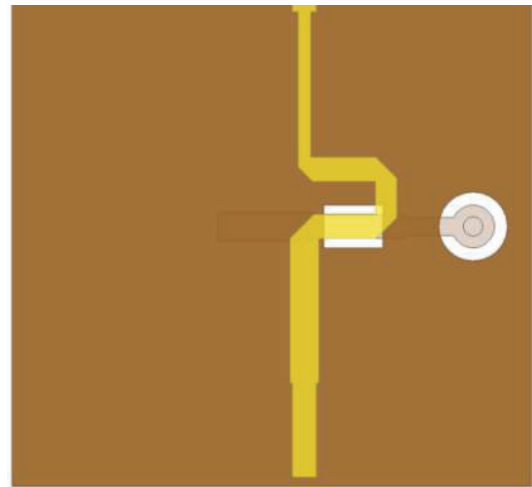


FIGURE 7. The coupling structure.



FIGURE 8. The series-fed calibration channel of the 1×8 antenna array.

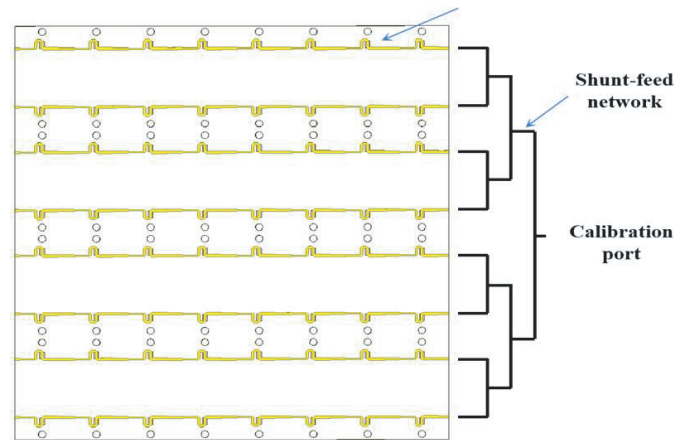


FIGURE 9. The schematic architecture diagram of the calibration channel for 8×8 antenna array.

lines. The calibration network is placed on Layer 3, while the antenna element is placed on Layer 13 to Layer 24. There is a ‘window’ between the the calibration network and RF feed line, which is realized by a design of a slot between them in Layer 2. Each channel of the calibration network couples energy from the “window”. The calibration channels in a 1×8 antenna subarray are formed by a series feeding network, and then combined with a shunt feeding network to form the calibration channels of the whole array, as shown in Fig. 8 and Fig. 9.

From the calibration port, the amplitude and phase information of each antenna element can be coupled. Based on this amplitude and phase information, the amplitude and phase of the signal that fed to the antenna element can be adjusted in real-time from the RF chip end to meet the beamforming requirements of the antenna array scanning beam [22, 23].

Layer No.	Layer description		Material	Board Thickness (mm)
Lay1	RF signal		TSM-DS3M	0.018
Lay2	GND		TSM-DS3M	0.127
			TSM-DS3M	0.018
			FR28 PP	0.1
Lay3	Calibration layer			0.018
Lay4	GND		TSM-DS3M	0.127
			TSM-DS3M	0.018
			FR28 PP	0.1
Lay5	Power divider			0.018
Lay6	GND		TSM-DS3M	0.127
			TSM-DS3M	0.018
			FR28	0.1
Lay7	AVDD			0.018
Lay8	GND		TSM-DS3M	0.127
			TSM-DS3M	0.018
			FR28	0.1
Lay9	DVDD			0.018
Lay10	GND		TSM-DS3M	0.127
			TSM-DS3M	0.018
			FR28	0.1
Lay11	Signal			0.018
Lay12	GND		TSM-DS3M	0.127
			TSM-DS3M	0.018
			FR28	0.1
Lay13	Power divider			0.018
Lay14	GND		TSM-DS3M	0.127
			TSM-DS3M	0.018
			FR28	0.1
Lay15	None			0
Lay16	GND		TSM-DS3M	0.127
			TSM-DS3M	0.018
			FR28 PP	0.1
Lay17	None			0
Lay18	Feeding network		TSM-DS3M	0.127
			TSM-DS3M	0.018
			FR28 PP	0.1
Lay19	None			0
Lay20	Radiation patch		TSM-DS3M	0.127
			TSM-DS3M	0.018
			FR28	0.1
Lay21	None			0
Lay22	None		TSM-DS3M	0.127
			TSM-DS3M	0
			FR28	0.1
Lay23	None			0
Lay24	Parasitic patch		TSM-DS3M	0.127
			TSM-DS3M	0.018
				2.948

FIGURE 10. Multilayer laminated PCB board design.

3.4. Integrated Design of RF Antenna

Phased array multi-channel transceiver chips are the key issues in high-integration applications. In this design, a silicon-based, eight-channel transceiver chip TW7205 is used. The chip can switch between receiving and transmitting modes through half duplex operation. The chip is embedded with power amplifiers, low noise amplifiers, attenuators, and phase shifters. Each channel signal supports amplitude adjustment with 5-bit accuracy in the range of 0–15.5 dB and phase adjustment with 6-bit accuracy in the range of 0–360°. The chip adopts FO_WLCSP packaging, with a size of 6 mm × 6 mm. To meet the requirements of miniaturization, high integration, and low cost in UAV applications, the millimeter wave active antenna adopts the AiP form. The system adopts multi-layer PCB and High Density In-

terconnector (HDI) process. The antenna elements are placed on the front of the PCB and multi-channel chips on the back. The entire AiP antenna adopts a 24 layers stacked design, including 12 layers for the antenna part and 12 layers for the antenna chip interconnection part [24, 25]. The stacked design is shown in Fig. 10.

The active antenna prototype is shown in Fig. 11.

4. TEST

4.1. Frequency Band Testing

To test the frequency band of the active antenna, the proposed active antenna is used as a transmitter, while a horn antenna and

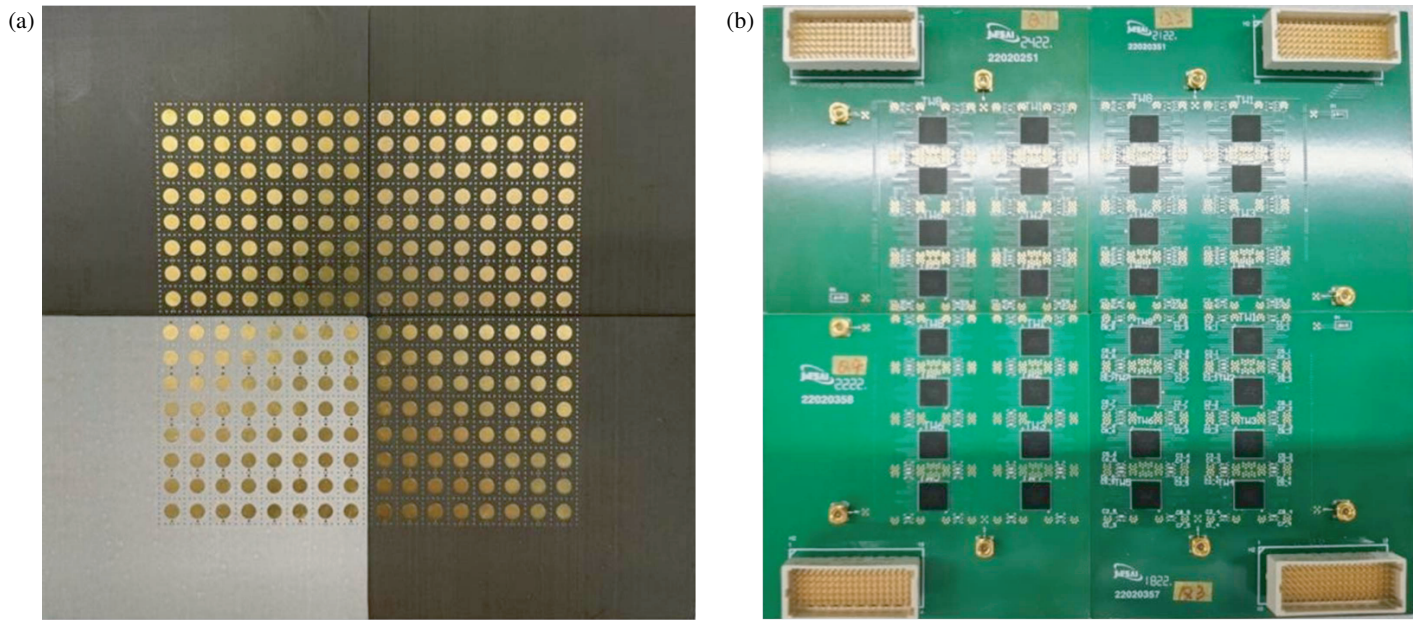


FIGURE 11. Prototype of integrated antenna and chip. (a) Front-antenna side. (b) Back-chip side.



FIGURE 12. Frequency band testing of the active antenna.

a vector network analyzer is used as a receiver. When the channels are open and closed, the antenna’s operating frequency range can be shown in the vector network analyzer. The test results are shown in Fig. 12, which meet the design frequency band 24.75–27.5 GHz requirements.

4.2. Communication Performance Testing

To verify the communication performance of the active antenna, the millimeter wave active antenna is connected to a frequency conversion module and a 5G millimeter wave base-band module. The receiver side uses a horn antenna and a signal analyzer to receive 5G millimeter wave standard signals. The signal demodulation performance is tested at the receiver

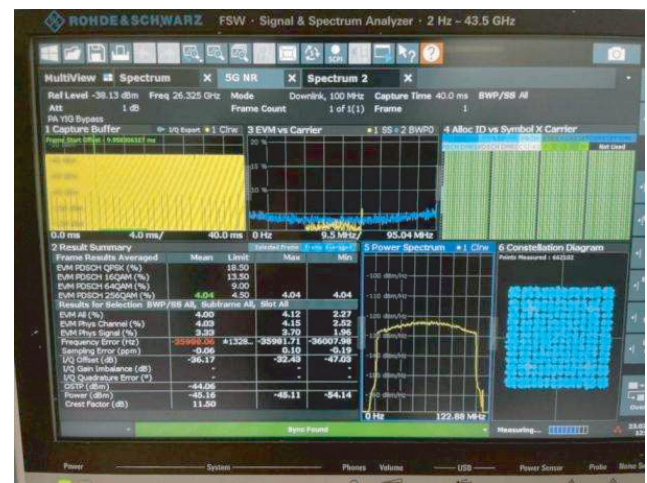


FIGURE 13. Active antenna communication performance testing.

side [26, 27]. Through testing, the antenna can achieve real-time demodulation of 100 MHz, 256QAM 5G millimeter wave signals, as shown in Fig. 13.

5. CONCLUSION

Focusing on the millimeter wave communication requirements of UAVs, this article designs and verifies a millimeter wave active antenna. The circularly polarized antenna designed through AiP meets the requirements of signal tracking and real-time information transmission during high-speed dynamic flight of UAVs. It has broad application prospects in UAV communication systems.

REFERENCES

- [1] Chittimoju, G. and U. D. Yalavarthi, "A comprehensive review on millimeter waves applications and antennas," in *Journal of Physics: Conference Series*, Vol. 1804, No. 1, 012205, 2021.
- [2] Zhang, L., H. Zhao, S. Hou, Z. Zhao, H. Xu, X. Wu, Q. Wu, and R. Zhang, "A survey on 5G millimeter wave communications for UAV-assisted wireless networks," *IEEE Access*, Vol. 7, 117 460–117 504, 2019.
- [3] Xiao, Z., K. Liu, and L. Zhu, "Millimeter-wave array enabled UAV-to-UAV communication technology," *Journal on Communications*, Vol. 43, No. 10, 196–209, Oct. 2022.
- [4] Fu, Z., J. Luo, J. Ning, *et al.*, "Application status and prospect of UAV swarm communications," *Radio Engineering*, Vol. 53, No. 1, 3–10, 2023.
- [5] Zhu, X. and X. Jin, "Research on millimeter wave ultra massive MIMO channel estimation," *Radio Communications Technology*, Vol. 49, No. 3, 404–409, 2023.
- [6] Xia, W., V. Semkin, M. Mezzavilla, G. Loianno, and S. Rangan, "Multi-array designs for mmWave and sub-THz communication to UAVs," in *2020 IEEE 21st International Workshop on Signal Processing Advances in Wireless Communications (SPAWC)*, 1–5, Atlanta, GA, USA, 2020.
- [7] Zhu, X. and X. Jin, "Research on millimeter wave ultra massive MIMO channel estimation," *Radio Communications Technology*, Vol. 49, No. 3, 404–409, 2023.
- [8] Xiao, Z., L. Zhu, Y. Liu, P. Yi, R. Zhang, X.-G. Xia, and R. Schober, "A survey on millimeter-wave beamforming enabled UAV communications and networking," *IEEE Communications Surveys & Tutorials*, Vol. 24, No. 1, 557–610, 2022.
- [9] Liu, K., Y. Liu, T. Mao, Z. Xiao, and X.-G. Xia, "Robust hybrid beamforming for jittering UAV with mmwave antenna array," in *2022 IEEE/CIC International Conference on Communications in China (ICCC)*, 244–249, Sanshui, Foshan, China, 2022.
- [10] Vaughan, R. G., "Polarization diversity in mobile communications," *IEEE Transactions on Vehicular Technology*, Vol. 39, No. 3, 177–186, 1990.
- [11] Wei, X., L. Peng, R. Xu, A. Li, X. Yu, and Z. Xu, "Performance optimization of UAV-assisted networks with mmWave antennas," in *2023 International Conference on Wireless Communications and Signal Processing (WCSP)*, 652–657, Hangzhou, China, 2023.
- [12] Xue, J., Y. Li, X. Shen, and H. Liu, "Ka-band highly integrated active phased array antenan design based on SIP," *Space Electronic Technology*, Vol. 20, No. 3, 84–88, Jun. 2023.
- [13] Asrizal, Y., A. Awaludin, and J. T. S. Sumantyo, "Low sidelobe and tilted beam microstrip antenna for circularly-polarized SAR onboard UAV," *Progress In Electromagnetics Research Letters*, Vol. 104, 95–103, 2022.
- [14] Su, J., B. Lin, H. Dou, and X. Chen, "A freely extendable closely packed dual-band MIMO antenna for 5G wireless communication," *Progress In Electromagnetics Research Letters*, Vol. 114, 21–29, 2023.
- [15] Cui, G., N. Liu, R. Song, and J. Liu, "A multi-point fed circularly polarized millimeter wave antenna element with π -shaped coupling apertures," in *Conference on Infrared, Millimeter, Terahertz Waves and Applications (IMT2022)*, Vol. 12565, 2023.
- [16] Liu, X., W. Zhang, D. Hao, and Y. Liu, "Cost-effective surface-mount patch antenna with ring slot using ball grid array packaging for 5G millimeter-wave applications," *Progress In Electromagnetics Research Letters*, Vol. 99, 127–133, 2021.
- [17] Liu, X., W. Zhang, D. Hao, and Y. Liu, "A 3743 GHz endfire antenna element based on ball grid array packaging for 5G wireless systems," *Progress In Electromagnetics Research Letters*, Vol. 99, 135–142, 2021.
- [18] Li, J., Z. Xiang, X. Chen, M. Xu, and J. Li, "Broadband bowtie-based log-periodic array antenna via GIPD process for 5G mm-Wave applications," *Progress In Electromagnetics Research Letters*, Vol. 118, 55–61, 2024.
- [19] Le, T. H., I. Ndip, O. Schwanitz, S. Kosmider, K. S. Murugesan, U. Maass, and M. Schneider-Ramelow, "Compact wideband antenna-in-package based on PCB technology for 39 GHz 5G mmwave applications," in *2022 16th European Conference on Antennas and Propagation (EuCAP)*, 1–4, Madrid, Spain, 2022.
- [20] Yang, Y.-H., B.-H. Sun, and J.-L. Guo, "A single-layer wideband circularly polarized antenna for millimeter-wave applications," *IEEE Transactions on Antennas and Propagation*, Vol. 68, No. 6, 4925–4929, Jun. 2020.
- [21] Li, J., X. Yu, Y. Yao, *et al.*, "A low-profile dual-polarized antenna in millimeter-wave band," *Radio Engineering*, Vol. 53, No. 8, 1760–1766, 2023.
- [22] Liu, Y., X. Zhang, and S. Zhou, "Joint real-time phase shifter network calibration and beam tracking for mmwave communication," *IEEE Wireless Communications Letters*, Vol. 10, No. 9, 1979–1983, Sep. 2021.
- [23] Hwang, I.-J., Y.-P. Hong, and J.-I. Park, "Element-level phase measurement and calibration of array antenna for mmWave 5G communications," in *2022 International Symposium on Antennas and Propagation (ISAP)*, 497–498, Sydney, Australia, 2022.
- [24] Shang, G., N. Liu, and G. Cui, "Broadband circularly polarized antenna based on multi-layer PCB technology for millimeter-wave applications," in *2022 International Conference on Microwave and Millimeter Wave Technology (ICMMT)*, 1–3, 2022.
- [25] Cui, G., N. Liu, R. Song, N. Zhang, G. Shang, and G. Yang, "A circularly polarized millimeter-wave antenna with high radiation efficiency," in *2022 IEEE 9th International Symposium on Microwave, Antenna, Propagation and EMC Technologies for Wireless Communications (MAPE)*, 256–259, 2022.
- [26] Lisi, M., "Specification, verification, and calibration of active electronically scanned array (AESA) antennas," in *2021 4th International Symposium on Advanced Electrical and Communication Technologies (ISAECT)*, 1–6, Alkhobar, Saudi Arabia, 2021.
- [27] Liang, B., L. Wang, H. Tu, *et al.*, "Research on high order modulation in UAV broadband data link," *Radio Engineering*, Vol. 52, No. 4, 544–549, 2022.